

IDENTIFICATION OF RESIDUES CRITICAL TO EPITHELIAL SODIUM
CHANNEL ASSEMBLY

Presented to the Graduate Council of
Texas State University-San Marcos
in Partial Fulfillment
of the Requirements

for the Degree

Master of SCIENCE

By

Ty E. Whisenant, B.A.

San Marcos, Texas
August 2011

IDENTIFICATION OF RESIDUES CRITICAL TO EPITHELIAL SODIUM
CHANNEL ASSEMBLY

Committee Members Approved:

Rachell E. Booth, Chair

Linette Watkins

Wendi David

Approved:

J. Michael Willoughby
Dean of the Graduate College

FAIR USE AND AUTHOR'S PERMISSION STATEMENT

Fair Use

This work is protected by the Copyright Laws of the United States (Public Law 94-553, section 107). Consistent with fair use as defined in the Copyright Laws, brief quotations from this material are allowed with proper acknowledgment. Use of this material for financial gain without the author's express written permission is not allowed.

Duplication Permission

As the copyright holder of this work I, Ty Whisenant, refuse permission to copy in excess of the "Fair Use" exemption without my written permission.

ACKNOWLEDGEMENTS

First and foremost, Dr. Rachell Booth deserves my utmost gratitude. The time that she committed to training and mentoring me were paramount to my success at Texas State. I cannot thank her enough for all of the advice and assistance that she has given me. The past two years in her lab will always be remembered upon as interesting, educational, and fun. I would also like to thank my committee members Dr. Wendi David and Dr. Linette Watkins for their helpful suggestions and support. Very special thanks go to Dr. Kevin Lewis for his expert recommendations in all yeast related quandaries that I encountered. I would like to acknowledge the staff and the rest of the faculty of the Chemistry & Biochemistry Department for creating such a great atmosphere for learning.

I would like to thank the entire Booth lab for making the lengthy experiments seem to go by so quick. I left the lab laughing or with a smile on my face every day. I would also like to thank Katelyn Gallier, Samantha Swann, and Roberta Rodrigues for their assistance in a number of experiments.

Finally, I would like to thank my family for supporting and encouraging me in all of my scientific and educational endeavors. I would especially like to thank Allison Tinsley. Your ever present support and love have been critical to my success. Thank you for tolerating all of the evenings and weekends spent in the lab. I am so grateful for you

being there with me as I continue my educational journey. I am very lucky to have someone like you.

This manuscript was submitted May 17, 2011.

TABLE OF CONTENTS

ACKNOWLEDGEMENTS	iv
LIST OF TABLES	vii
LIST OF FIGURES	viii
ABSTRACT	ix
CHAPTER	
I. INTRODUCTION AND LITERATURE REVIEW	1
II. MATERIALS AND METHODS.....	9
III. RESULTS AND DISCUSSION.....	16
IV. CONCLUSIONS.....	38
REFERENCES	41

LIST OF TABLES

Table	Page
1: Custom primers for EP-PCR random mutagenesis.....	11
2: Custom primers for sequencing mutants	15
3: EP-PCR conditions	20
4: Total phenotype observations for EP-PCR conditions	25
5: Summary of mutants, EP-PCR conditions, and amino acid transition	35

LIST OF FIGURES

Figure	Page
1: Conserved domains of ENaC/DEG family members	3
2: ENaC regulation	4
3: Pronging of homomeric and heteromeric ENaC.....	17
4: Vector map of pYES2N/T	18
5: Digestion of pYES2NT/A – alpha ENaC by BclI and BssHIII	19
6: Gel electrophoresis of EP-PCR products.....	21
7: Outline of genetic recombination process in <i>S. cerevisiae</i>	22
8: Co-transformation into <i>S. cerevisiae</i>	23
9: Pronging assay of pYES2NT/A with and without alpha ENaC	24
10: Dilution pronging assay of mutants and corresponding phenotype.....	25
11: Gel electrophoresis of DNA isolated from <i>S. cerevisiae</i>	26
12: pYES2NT/A – alpha ENaC mutants transformed into <i>E. coli</i>	28
13: Digestion of mutant pYES2NT/A – alpha ENaC by ClaI and AgeI	29
14: Pronging assay of each EP-PCR condition and point mutations	30
15: Alignment of sequenced mutant plasmids	31
16: Model of human alpha ENaC based on the ASIC1 crystal structure.....	36

ABSTRACT

IDENTIFICATION OF RESIDUES CRITICAL TO EPITHELIAL SODIUM CHANNEL ASSEMBLY

by

Ty E. Whisenant

Texas State University-San Marcos

August 2011

SUPERVISING PROFESSOR: RACHELL E. BOOTH

The Epithelial Sodium Channel (ENaC) is a major determinant in fine-tuning the volume and pressure of blood within the cardiovascular system. An understanding of the regulation, structural assembly, and arrangement of ENaC is needed. This study describes a method for identifying residues that participate in structural stability interactions between and within subunits as well as those critical to function. A novel yeast screen

was used to describe salt-sensitive phenotypes observed in *S. cerevisiae* that showed growth inhibition after expression of ENaC. Error prone polymerase chain reaction (EP-PCR) was employed to promote random mutagenesis in the extracellular loop of alpha-ENaC. The levels of growth inhibition were monitored in the yeast strain S1InsE4A transformed with mutant alpha ENaCs and these mutants were subsequently characterized. The location of the point mutations within the primary protein sequence of alpha ENaC and the corresponding amino acid transitions caused varying degrees of growth inhibition (i.e. function). This study successfully illustrates a method for inducing mutations in an area of interest and screening the resulting mutants for changes in functions. Using this methodology, we identified several residues within the extracellular domain of alpha ENaC that are critical for function.

CHAPTER I

INTRODUCTION AND LITERATURE REVIEW

The human body contains an interconnected network of mechanisms designed to keep a homeostatic equilibrium of water, solutes, and other solvents within an optimum range for favorable physiological conditions. The circulatory system requires blood pressure, and thus water and solute concentrations, to be constantly regulated at the epithelial cells of the kidneys for homeostasis. The pulmonary epithelia require proper osmolality of the surrounding fluid for optimal respiratory functionality. Fine adjustments to these systems can be made by up or down regulating ENaC, which is responsible for sodium re-absorption in the distal tubules of the nephron, lungs, and large intestines.

ENaCs are identified as voltage independent, constitutively open, amiloride-sensitive channels located in the apical membrane of epithelial cells. Sodium regulation due to ENaC is accomplished mainly through the distal tubule of the nephron within the kidneys, which is located between the loop of Henle and the collecting duct. Unfiltered blood from the circulatory system reaches the glomerulus via the afferent arteriole. The blood is filtered through Bowman's capsule and is processed into what will ultimately be

urine. The filtrate is conveyed through the nephron simultaneously having ions and compounds reabsorbed into the bloodstream. Once the filtrate reaches the distal tubule of the nephron, the ENaC extracellular region which extends into the lumen of the tubule will absorb sodium from the urine into the epithelia through passive transport at a rate based on the concentration gradient. As the sodium concentration increases within the epithelial cells, another transport protein is employed to release the ions into the blood stream. The potassium/sodium-ATPase antiporter is located in the basolateral membrane of epithelia and moves two potassium ions from the blood stream across the membrane into the cells opposite the transport of three sodium ions. The ATPase pump, unlike ENaC, uses active transport as a mechanism for movement of ions during which the enzyme undergoes various conformation changes due to substrate and cofactor binding (1). Water molecules follow the ions through the permeable cells and into the blood resulting in a higher volume and increased blood pressure.

ENaC is a member of the ENaC/degenerin (ENaC/DEG) gene superfamily (2). ENaC and acid-sensing ion channels (ASICs) in animals are two sub-families of the diverse ENaC/DEG protein family. There are highly conserved regions amongst members, including cysteine-rich domains (CRDs) and two transmembrane domains (M1, M2) (Figure 1A). A common attribute that is conserved throughout this ion channel family is an extracellular loop, containing conserved CRDs, that connects M1 and M2 (Figure 1B). There is a universal topology throughout the family in which the N-terminal and C-terminals are both intracellular.

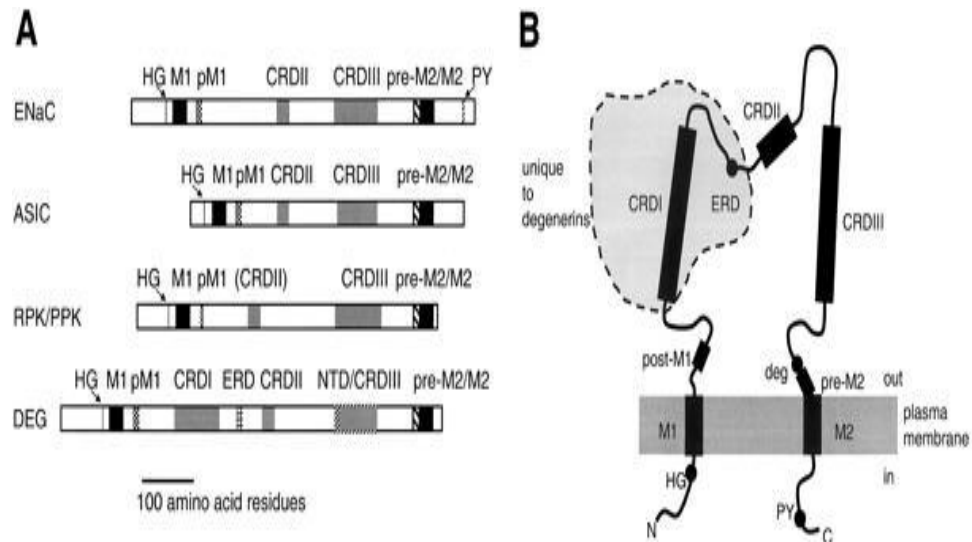


Figure 1: Conserved domains of ENaC/DEG family members. (A) Homologous regions compared between ENaC/DEG family members. (B) Topology of an individual ENaC/DEG subunit. The shaded gray region of CRDI and ERD are unique to degenerins (3).

Typically, the ENaC is composed of the following three subunits: alpha, beta, and gamma. Each individual subunit is coded from a separate gene, SCNN1A, SCNN1B, and SCNN1G, respectively. ENaC subunit stoichiometry has been shown to be in an equal ratio of alpha to beta to gamma using total internal reflection fluorescence studies (4). Furthermore, ENaC structure is likely in a stoichiometric fashion of 1 alpha, 1 beta, and 1 gamma which can be corroborated by recent research that considers the closely related ASIC1 protein to ENaC (5). The structure must be conjectured for the reasons that ENaC expression is at low levels making it difficult to purify adequate amounts needed for forming a crystal structure and that the transmembrane domains are highly hydrophobic which leads to aggregation and misfolding in purification. Alpha ENaC alone is capable of forming functional channels (6). Although, the homotrimer

demonstrates lower levels of sodium reabsorption compared to the heterotrimeric complex (7). Unlike the alpha subunit, beta and gamma, alone or combined with each other, cannot form a channel with notable function unless the alpha subunit is part of the heterotrimer. This unique property of alpha ENaC may account for the greater abundance of it compared to the other subunits at the cell surface when quantified in *Xenopus* oocytes (8). This property has also led to the hypothesis that the alpha subunit forms the core of the channel and the β and γ subunits act in an auxiliary fashion (9). Although functional homomeric protein formation is possible, it is rarely found in nature. This fact is based on electrophysiological studies where heteromeric protein structure is highly favored over homomeric structure when all three subunits are expressed (4).

ENaC is characterized as non-voltage gated and non-ligand gated. The lack of external stimuli controls makes the regulation of ENaC critical in maintaining sodium homeostasis. ENaC positioning at the apical membrane is regulated by the peptide hormone vasopressin, the steroid hormone aldosterone, and Nedd4 (Figure 2).

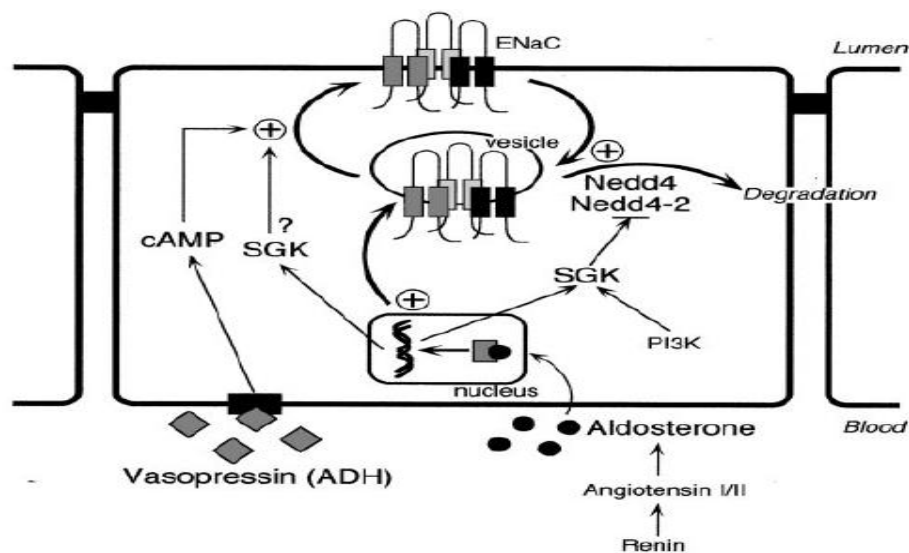


Figure 2: ENaC regulation. Vasopressin and Aldosterone promote ENaC exocytosis and transcription, respectively. Nedd4 assists ubiquitination of ENaC. (10)

The mechanisms that are known to instigate ENaC up-regulation are based primarily on the recognition of changes in osmotic pressure and the resulting response by hormone secretion of vasopressin and aldosterone in humans. Osmoreceptors in the hypothalamus detect an altered state of osmotic pressure by expanding or contracting based on the amount of water movement to or from the cell (11). Low osmotic pressure (low solute concentration) of the body's blood supply results in a signal being sent to the pituitary gland which releases vasopressin destined for the kidney (12). Vasopressin binds to receptors on basolateral membrane which activate a cAMP pathway (13). Protein Kinase A (PKA) is activated by increased cAMP concentrations and has been shown to subsequently assist soluble N-ethyl-maleimide-sensitive factor attachment protein receptors (SNARE) and complexin in the exocytotic trafficking of ENaC within cytoplasmic vesicles to the apical membrane (14). Additionally, vasopressin stimulates aquaporin-2 insertion to the apical membrane which allows more water to follow the sodium ions being transported across epithelia to assist an increase in blood pressure (15). Aldosterone is a mineralcorticoid protein hormone that also promotes up-regulation of ENaC. Aldosterone is excreted as the final product in the renin-angiotensin cascade that responds to hyponatremia. Renin is a peptide hormone that is excreted by granular cells in the juxtaglomerular apparatus. Renin acts as a protease by activating angiotensin I which is later converted to angiotensin II by angiotensin converting enzyme (ACE) and consequently induces release of aldosterone from the adrenal cortex. Aldosterone binds to extracellular receptors on epithelial cells and is transported to the nucleus where the complex promotes ENaC mRNA transcription (16, 17). Aldosterone also promotes transcription of Serum- and Glucocorticoid-regulated Kinase I (SGKI) which has been

shown to phosphorylate Nedd4-2, an ubiquitin ligase that targets ENaC in the apical membrane for degradation, and hinders its ability to recognize ENaC, thus allowing for more ENaC to be present and functional at the cell surface (18, 19). Recent studies have shown the 14-3-3 protein isoform 14-3-3 β is induced by aldosterone and interacts with phosphorylated Nedd4-2 to obstruct its interaction with ENaC in a similar fashion as SGK1 (20).

Renal A6 epithelial cells were used to determine that protein kinase C (PKC) inhibits ENaC channel activity (21). PKC has been determined to promote beta and gamma subunit degradation instead of affecting synthesis because of additional effects on channel activity when combined with transcription (actinomycin D) and translation (emetine and cycloheximide) inhibitors (22). Nedd4 regulates ENaC by selective ubiquitination of the intracellular C-terminus that contains PY regions for binding (23). Ubiquitination is a posttranslational modification that codes for degradation of the proteins tagged with ubiquitin, a polypeptide made of 76 amino acids (24). The culmination of the elements presented above is the basic down regulation of ENaC (Fig 2).

The number of channels present in the membrane and the length of time they are positioned there determine the rate of sodium intake activity for the cell. ENaC production and degradation are important influencing elements for channel quantity and life span. Therefore, any errors in the assembly or degradation mechanisms could cause major implications to physiological well-being.

Subtle changes in ENaC regulation mechanisms can be the source of physiological disease states observed in humans such as Pseudohypoaldosteronism I (PHA I) and Liddle's syndrome which cause hypotension and hypertension, respectively (25). Additionally, improper ENaC control may contribute to respiratory distress in cases of cystic fibrosis (26). PHA I can cause varying degrees of distress from being asymptomatic to life threatening occurrences of salt loss observed in infancy (27). PHA I can present itself with fainting, dizziness, and/or weakness from chronic hypotension. Patients have a continuous state of low blood pressure which keeps the brain, heart, and other organs from receiving a sufficient supply of blood. PHA I is caused by an inactive mutation that leaves ENaC unable to act in response to aldosterone. This leaves the epithelia without the adequate quantity of ENaC required for proper homeostasis and an excessive level of aldosterone. Salt wasting ensues from the inability to re-absorb proper amounts of sodium from the urine. Contrarily, Liddle's syndrome usually presents in infancy with severe hypertension which can cause renal failure, heart failure, strokes, and/or arterial aneurisms. Liddle's syndrome is caused by a mutation in the ENaC domain that is normally recognized by Nedd4. With Nedd4 unable to distinguish the PY motif, the lifetime of ENaC becomes prolonged which leads to an increase in sodium re-absorption and accordingly high blood pressure. Patients will either have normal or low levels of aldosterone. These genetic diseases demonstrate the physiological importance of ENaC.

This study seeks to find residues involved in inter-subunit interactions between the subunits of homomeric alpha ENaC to give a better understanding of ENaC's structure/function relationships. Using error-prone PCR (EP-PCR) random mutations in

ENaC can be generated and then screened for loss of function by a yeast pronging assay. Mutations of interest can then be characterized by evaluating a recent homology model between ENaC and a close protein family member by Stockand *et al.* as well as previously discerned critical residues in literature.

CHAPTER II

MATERIALS AND METHODS

Heat Shock Transformation of Plasmid DNA into *E. coli*:

One hundred microliters of competent *E. coli* cells were mixed with 100 ng of isolated plasmid on ice for 20 minutes. Next, the reaction mixture was incubated at 42°C for 45 seconds and then on ice for 2 minutes. One milliliter of LB broth was added to the mixture and incubated at 37°C with shaking for 60 minutes. Fifty microliters to 500 µL aliquots of the mixture were spread onto a LB plate containing 100 µg/mL ampicillin and allowed to incubate overnight at 37°C.

Isolation of Plasmid DNA from *E. coli*:

A single, isolated colony of transformed *E. coli* was incubated overnight at 37°C with shaking in 5 mL of LB Broth from Becton Dickinson (Sparks, MD) supplemented with 100 µg/mL ampicillin. After 16 to 24 hours of growth, 800 µL of the mixture was removed and used to make a glycerol stock for further experimentation. Three milliliters of culture was used for isolation of plasmid as per the manufacturer's protocol of the Qiagen QIAprep Spin Miniprep kit (Valencia, CA). Cell lysis solutions, centrifugation of

lysates, and isolation via chromatographic columns are utilized in the protocol. Plasmid was eluted in sterile water instead of TE buffer so as not to interfere with subsequent experimentation. Eluted plasmid was confirmed for presence of pYES2NT/A – alpha ENaC or its mutants by horizontal gel electrophoresis and quantitated in a Nanodrop ND-1000 Spectrophotometer from Thermo Fisher Scientific (Wilmington, DE).

Horizontal Gel Electrophoresis:

Fifty milliliter, 1.0% w/v agarose slab gels were prepared using 1X TAE Buffer (40 mM Tris-base, pH 8, 20 mM acetic acid, 1 mM EDTA). Gels were placed in a QS710 Horizontal Gel Electrophoresis Unit from Shelton Scientific (Shelton, CT) and enough 1X TAE Buffer was added to cover the slab. Samples of plasmid were mixed with 1X Endorstop (10 mM EDTA, 5% v/v glycerol, 0.1% w/v SDS, 0.01% w/v bromophenol blue, pH 8.0). The samples were loaded into the gel and electrophoresis proceeded for 50 to 60 minutes at 110 volts. The gel was then stained with 0.2 mg/mL ethidium bromide solution for 30 minutes, rinsed in ddH₂O for 30 minutes, and imaged with Alpha Innotech Red Gel Imaging System (Santa Clara, CA).

EP-PCR:

The reaction mixtures consisted of 100 ng of DNA, 1 μM custom primers, 1X Thermopol buffer, 1 unit of Taq Polymerase, 0.5 mM dNTP, and ddH₂O to 50 μL. Alternatively, experiments used a NEB 1X Mastermix with primers, dNTP, and Taq

Polymerase. Various amounts of MgCl₂ (0.0 to 4.5 mM final concentrations) and MnCl₂ (0.0 or 0.5 mM final concentrations) were added in multiple combinations. The reactions were carried out in an Applied Biosystems 2720 Thermo Cycler under the following run conditions: 94°C for 2 minutes, twenty-five cycles of 94°C for 30 seconds, 60°C to 55°C for 30 seconds, and 72°C for 60 seconds. The annealing temperature changed 1°C every five cycles. Once the PCR reaction was complete, 5 µL of the reaction mixture was analyzed with horizontal gel electrophoresis.

Table 1: Custom primers for EP-PCR random mutagenesis

Primer Name	Primer Sequence
AlphaRandomMutForward	5'-AAATACAACCTCTTCCTACACTCGCCAGGCT-3'
AlphaRandomMutReverse	5'-AGGCAGCCTGCAGTTTATAGTAGCAGTAGC-3'

EP-PCR Cleanup:

PCR product cleanup was performed on the reaction mixture (approximately 45 µL) using a Promega Wizard PCR Preps DNA Purification System following the protocol provided. Protocol details include use of solution to bind plasmid to centrifuge columns, wash solutions to elute contaminants, and elution of product with ddH₂O.

Digestion alpha-ENaC:

The restriction enzyme BclI is blocked by dam methylation which required the plasmid to be grown in a dam(-) strain of *E. coli*, ER2925 (NEB). Digestion reactions included 6 µg of DNA, 6 units of each restriction enzyme (BclI and BssHII), 1X NEB buffer 3, and ddH₂O to 50 µL. The digestion reaction was carried out for two hours at 50°C and stopped with 1X Endorstop. The digestion products were analyzed using horizontal gel electrophoresis.

Gel Extraction:

The digestion product bands of interest were extracted and cleaned using Promega Wizard PCR Preps DNA Purification System (Madison, WI) following the protocol provided. Bands of interest were identified using UV light and excised. The excised gel was incubated with a binding solution at 60°C then purified with a column. Multiple wash solutions were employed for contaminant removal and final product was eluted with ddH₂O.

Genetic Recombination of EP-PCR Product and Digestion Product:

S. cerevisiae S1InsE4A was incubated in YPDA broth (1% w/v yeast extract, 2% w/v peptone, 0.02% adenine, and 2% w/v glucose) for 16-20 hours at 30°C with shaking. The mixture was centrifuged on a Beckman Coulter Microfuge 18 centrifuge (Fullerton, CA) for 30 seconds at maximum speed and the supernatant was discarded. Next, the cell

pellet was resuspended in 1 mL of ddH₂O by vortexing on a VRW MiniVortexer MV1 (Batavia, IL) at maximum speed. The mixture was centrifuged and the supernatant was discarded again. The pellet was re-suspended in 1 mL of 0.1 M lithium acetate, centrifuged, and the supernatant was discarded again. The pellet was resuspended in 240 µL polyethylene glycol 4000 molecular weight, 0.5 M lithium acetate, 5 µg of sonicated salmon sperm (Stratagene), 400 ng of EP-PCR product, 400 ng of digested plasmid, and ddH₂O to 70 µL. The transformation was allowed to incubate at 30°C for 30 minutes with shaking. The mixture was then transferred to a 42°C and incubated for 20 minutes. Next, the mixture was centrifuged at maximum speed and the supernatant was discarded. The pellet was resuspended in 750 µL of ddH₂O. Two hundred fifty microliter and 500 µL aliquots of the mixture was spread onto 2% glucose minus Ura plates containing 100 µg/ml ampicillin and incubated at 30°C. Successful transformations were used to make patch plates for further experimentation.

Pronging Assay:

Samples of yeast were obtained from patch plates and resuspended in 0.5 mL of ddH₂O and prepared into 1/40 dilutions. Dilutions were subjected to sonication for six to eight seconds at two to four watts using Sonics Vibracell Ultrasonic Processor (Newtown, CT) to ensure cell separation. A Reichert hemocytometer (Buffalo, NY) was employed to quantitate the cells under a Comcon LOMO phase contrast microscope. Two hundred twenty microliter aliquots containing a standardized cell amount of 1×10^7 , based on hemocytometer counts, were added to a sterile 96-well plate and subjected to a

five-fold serial dilution across half the length of the plate. Cells were then pronged onto either 2% glucose or 2% galactose agar plates containing various amounts of salt concentrations from 0.0 to 1 M NaCl. The pronging plates were incubated at 30°C for two to six days until sufficient growth was visible for salt sensitive phenotype characterization.

Isolation of Mutant Plasmid from *S. cerevisiae*:

Liquid selective media was inoculated with a single colony and incubated for 16-20 hours at 30°C with shaking. Plasmids were isolated from *S. cerevisiae* using the USB PrepEase Yeast Plasmid Isolation Kit (Cleveland, Ohio) according to the manufacturer's protocol. The procedure made use of an enzyme solution to break down the yeast cell wall and buffer for the resultant spheroplasts. A lysis solution was used to disrupt the spheroplasts and the non-genomic portions are subsequently precipitated. Centrifugation was used to compact the cellular debris. Genomic and plasmid DNA contained in the supernatant were precipitated with ethanol and resuspended in ddH₂O.

Digestion of EP-PCR Mutant Plasmid:

To confirm proper genetic recombination within *S. cerevisiae* the isolated plasmids were subjected to restriction digestion with AgeI and ClaI. Six units of each restriction was added to 6 µg of plasmid DNA with ddH₂O to 50 µL and incubated at

37°C for 90 minutes. The reactions were stopped by addition of 1X Endorstop. Digestion products were run on horizontal gel electrophoresis for verification.

Sequencing of Mutant Plasmid:

Samples containing 400-500 ng/mL of isolated plasmid DNA in ddH₂O and 3 μM of custom primers were delivered to Davis Sequencing (Davis, CA). Reactions were performed with ABI 3730 sequencers using Applied Biosystems Big Dye V3.0 sequencing chemistry. The sequences were checked for mutations by comparison to known sequences.

Table 2: Custom primers for sequencing mutants

Primer Name	Primer Sequence
MutantSequencingForward	5'-CTTCGGCATGATGTACTGGC-3'
MutantSequencingReverse	5'-TTGAGTAGCCAGCAGAGAGC-3'

Chapter III

RESULTS AND DISCUSSION

In an endeavor to identify residues that are critical to inter-subunit interactions of ENaC, we based our experiments on the fact that alpha ENaC assembles into a functional homotrimeric protein. Residues that provide stability between the three alpha subunits may be homologous to residues that stabilize the heterotrimer subunits. We hypothesized that using EP-PCR to produce random mutagenesis would cause an amino acid transition on residues that are responsible for proper assembly of the subunits. If residues that interact with neighboring subunits by noncovalent or covalent bonding were mutated this would cause loss of function to varying degrees based on the importance of that interaction to overall protein architecture. The mutations may also have caused a loss of intra-subunit stability resulting in similar loss of function. Previous research in our lab has shown that gain or loss of ENaC function can be visualized by a yeast dilution pronging assay. We utilized the genetic recombination mechanisms present in yeast in conjunction with EP-PCR to produce ENaC containing mutations in the extracellular loop. Sequences were then compared to the wild-type nucleotide and peptide sequences to assess the relevance of each mutation to structure or functional change.

Pronging Assay of Multiple ENaC Stoichiometries

In order to determine the validity of using alpha only ENaC for future functional investigations, preliminary experiments consisted of co-transformation of vectors containing genes for each of the three ENaC subunits into *S. cerevisiae* in different combinations. A dilution pronging assay was utilized to determine the salt-sensitive phenotypes of the different homo- and heteromeric combinations (Figure 3). The heteromeric combinations showed greater growth inhibition in the alpha beta gamma stoichiometry and decreasing sensitivity for the alpha gamma, alpha beta, and alpha-only combinations, respectively. Alpha-only ENaC displays a phenotype unique from the negative control and will be used as a model for future studies. The phenotype patterns were similar for assays performed in 1.0 M NaCl and 0.1 M NaCl (data not shown), thus, future experiments used 0.1 M NaCl to assay variations in salt-sensitivity.

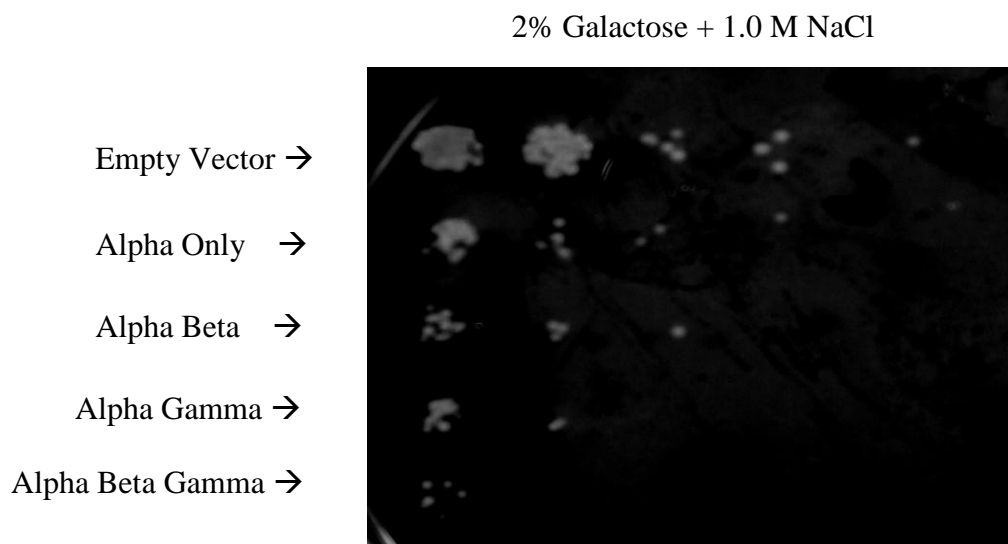


Figure 3: Pronging of homomeric and heteromeric ENaC. *S. cerevisiae* cells expressing various subunits of ENaC pronged onto 2% galactose + 1.0 M NaCl agar plate.

pYES2NT/A Vector

Alpha ENaC was previously subcloned into pYES2NT/A by Raquel Ybanez (Figure 4). The vector contained a feature that allowed controlled expression of alpha ENaC by a galactose promoter. In addition, the expression vector was utilized for its conveyance of resistance to ampicillin in bacteria and an auxotrophic gene for uracil when expressed in yeast. The Xpress epitope was used for detection of protein in Western blots. The C-terminal tags were not expressed due to possible disruption during trafficking of ENaC to the cell surface based on previous studies in our lab (unpublished results).

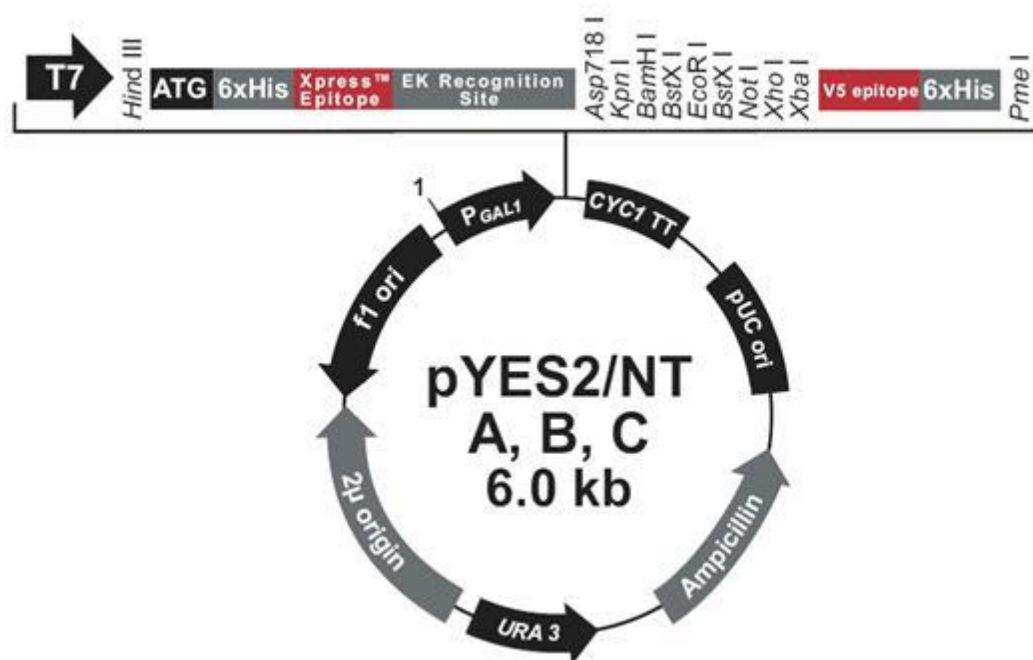


Figure 4: Vector map of pYES2N/T.

Digestion of alpha ENaC

In order to perform the genetic recombination, the sub-cloned alpha ENaC in pYES2NT/A was digested with BssHII and BclI. The plasmid was amplified in ER2925 *E. coli*. The digestion proceeded for 2 hours at 50 °C and the products were analyzed by gel electrophoresis for two expected fragments at 667 base pair and ~7.5 kb (Figure 5). The supercoiled, uncut plasmids were determined to be 6 kb as expected. The digested plasmids were subsequently extracted from the gel and purified using the Promega Wizard PCR Preps DNA Purification System. Plasmid concentration was quantitated in a Nanodrop ND-1000 Spectrophotometer with normal yields between 50 ng/μL and 150 ng/μL showing significant loss of plasmid through purification as was expected.

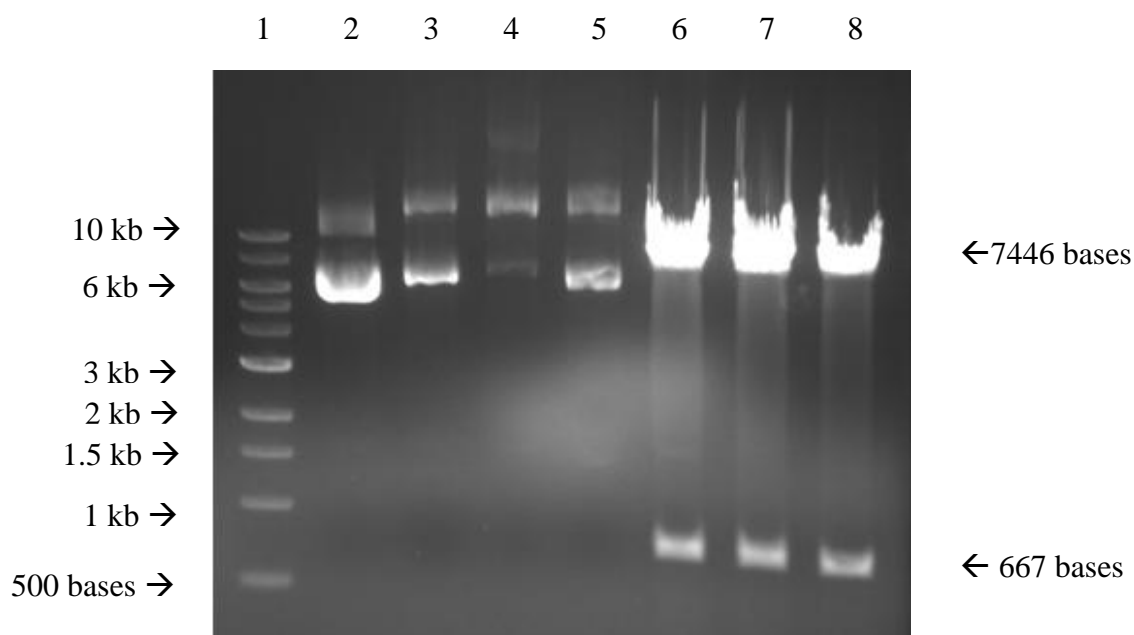


Figure 5: Digestion of pYES2NT/A – alpha ENaC by BclI and BssHII. 1% Agarose gel in 1X TAE Buffer stained with Et Br. Lane 1- 1 kb DNA ladder, Lane 2- control uncut pYES2NT/A – alpha ENaC, Lanes 3,4,5- uncut pYES2NT/A – alpha ENaC from ER2925, Lanes 6,7,8- digested pYES2NT/A – alpha ENaC from ER2925.

EP-PCR

The EP-PCR primers were designed to be 75 to 100 bases outside of the digested pYES2NT/A – alpha ENaC product to assist the genetic recombination mechanism in *S. cerevisiae*. EP-PCR was performed with the varied conditions seen in Table 3. Increased concentration of magnesium divalent cations alone or combined with manganese divalent cations were used to create products with various numbers of mutations.

Table 3: EP-PCR conditions

Reaction	#1	#2	#3	#4	#5	#6
25 mM MgCl ₂	1.5 mM	3 mM	4.5 mM	1.5 mM	3 mM	4.5 mM
5 mM MnCl ₂	0.0 mM	0.0 mM	0.0 mM	0.5 mM	0.5 mM	0.5 mM
DNA	100 ng					
Forward Primer	0.2 μM					
Reverse Primer	0.2 μM					
NEB Mastermix	1X	1X	1X	1X	1X	1X
ddH ₂ O for Total Volume	50 μL					

The thermocycler was set to perform a “touchdown” reaction during which the annealing temperature is lowered one degree Celsius per cycle. This helps to improve the efficiency of the reaction by increasing the probability of proper primer and template binding. PCR products were directly purified after the reaction using Promega Wizard PCR Preps DNA Purification System remove contaminants such as primer-dimers. The EP-PCR products were then analyzed by gel electrophoresis to confirm a 909 base pair fragment (Figure 6).

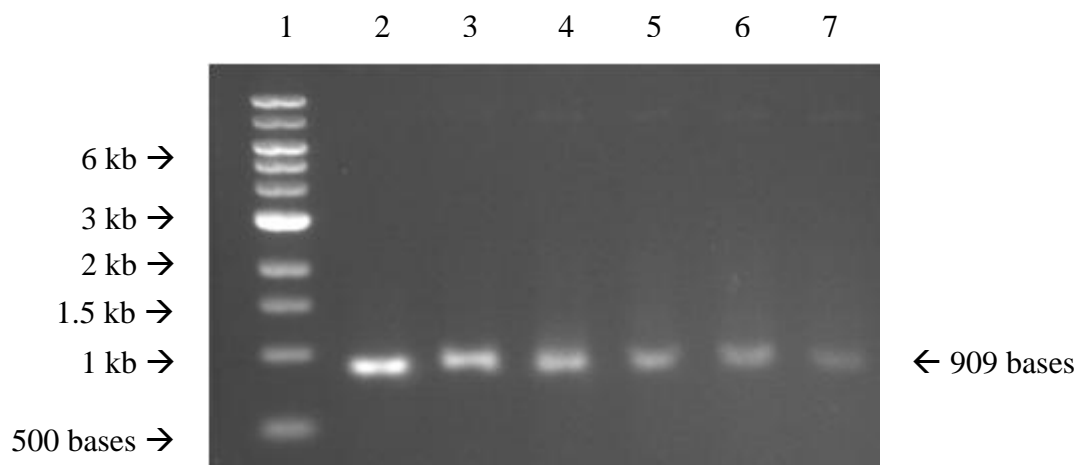


Figure 6: Gel electrophoresis of EP-PCR products. 1% Agarose gel in 1X TAE Buffer stained with Et Br. Lane 1- 1 kb ladder, Lane 2- Reaction 1, Lane 3- Reaction 2, Lane 4- Reaction 3, Lane 5- Reaction 4, Lane 6- Reaction 5, Lane 7- Reaction 6.

Genetic Recombination in *S. cerevisiae*

EP-PCR products and digested pYES2NT/A – Alpha ENaC in a ~10:1 molar concentration ratio were transformed via the high efficiency protocol into competent *S. cerevisiae* cells. Yeast has an uncanny ability to recombine PCR products with digested plasmids (Figure 7) by use of its natural DNA repair mechanisms provided there are homologous overlapping ends of lengths around 75 to 125 bases (28). Though, it has been shown that recombination will occur with overlapping sequences as short as 15 bases, but with a much decreased rate of success (29).

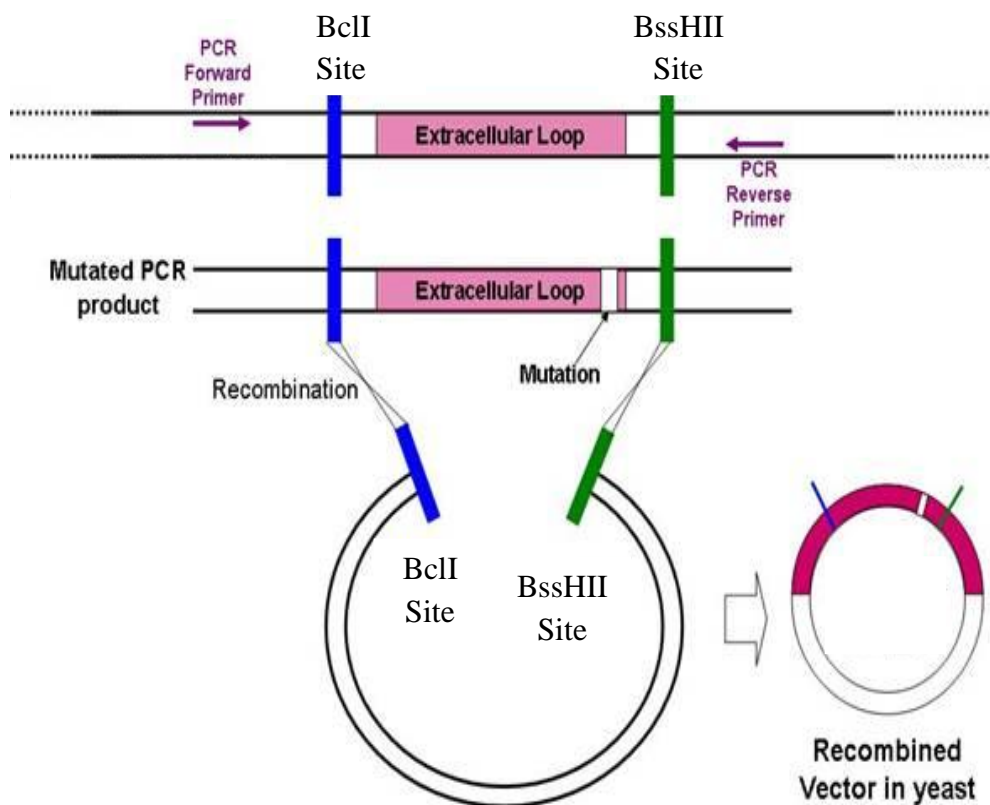


Figure 7: Outline of genetic recombination process in *S. cerevisiae*.

The transformed yeast cells were then spread on 2% glucose minus Ura agar plates and incubated overnight at 30°C. The transformation was consistently successful yielding over one hundred colonies for every EP-PCR reaction condition (Figure 8). Single, well isolated colonies were chosen for phenotype characterization by dilution pronging assay.

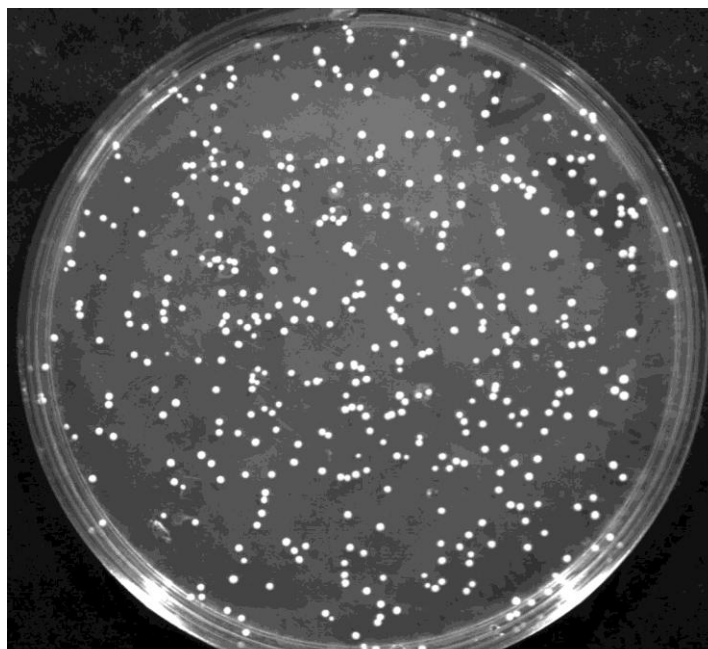


Figure 8: Co-transformation into *S. cerevisiae*. pYES2NT – alpha ENaC mutants from one EP-PCR reaction condition in yeast on 2% glucose minus Ura agar plate.

Pronging Assay of Random Mutations

To determine the functionality of mutated pYES2NT/A – alpha ENaC yeast colonies containing plasmids from each EP-PCR reaction were pronged onto synthetic media containing 2% glucose or 2% galactose supplemented with 0.1 M NaCl or 1.0 M NaCl. When grown on glucose, alpha ENaC was not expressed. Consequently, the yeast did not experience a dramatic increase in sodium absorption and grew normally regardless of mutations. The galactose media induced expression of the protein which was placed at the cell wall and allowed sodium uptake, if functional. The excess intracellular sodium caused growth inhibition of the yeast cells making visual verification quite simple. Initial experiments contained samples of S1InsE4A lacking pYESNT/A as a

negative control and S1InsE4A transformed with pYES2NT/A – alpha ENaC as a positive control (Figure 9).

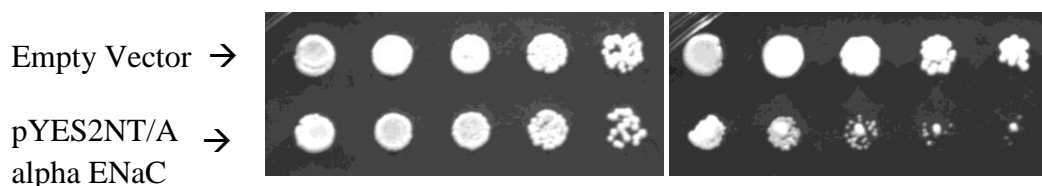


Figure 9: Pronging assay of pYES2NT/A with and without alpha ENaC. The empty vector (negative control) shows no growth inhibition on galactose or glucose salt-rich synthetic media. Salt sensitivity is shown for pYES2NT/A – alpha ENaC (positive control).

Later experiments contained only the positive control. Forty one observations of phenotypes from pronging to 2% galactose + 0.1 M NaCl involving the different EP-PCR conditions were studied in total (Table 4). *S. cerevisiae* expressing fully functional alpha ENaC displayed intense growth inhibition similar to the pYES2NT/A – alpha ENaC control and alpha mutant 13 (Reaction 4). The yeast cells that contained non-functional proteins, such as alpha mutants 14 (Reaction 4) and 15 (Reaction 5), possessed a salt insensitive phenotype and grew normally (Figure 10). Colonies that expressed reduced functional ENaC due to mutagenesis, such as alpha mutants 16 (Reaction 6) and 17 (Reaction 6), experienced decreased sensitivity to the salt-rich media. Forty one observations of phenotypes from pronging to 2% Galactose + 0.1 M NaCl involving the different EP-PCR conditions were studied in total (Table 4).

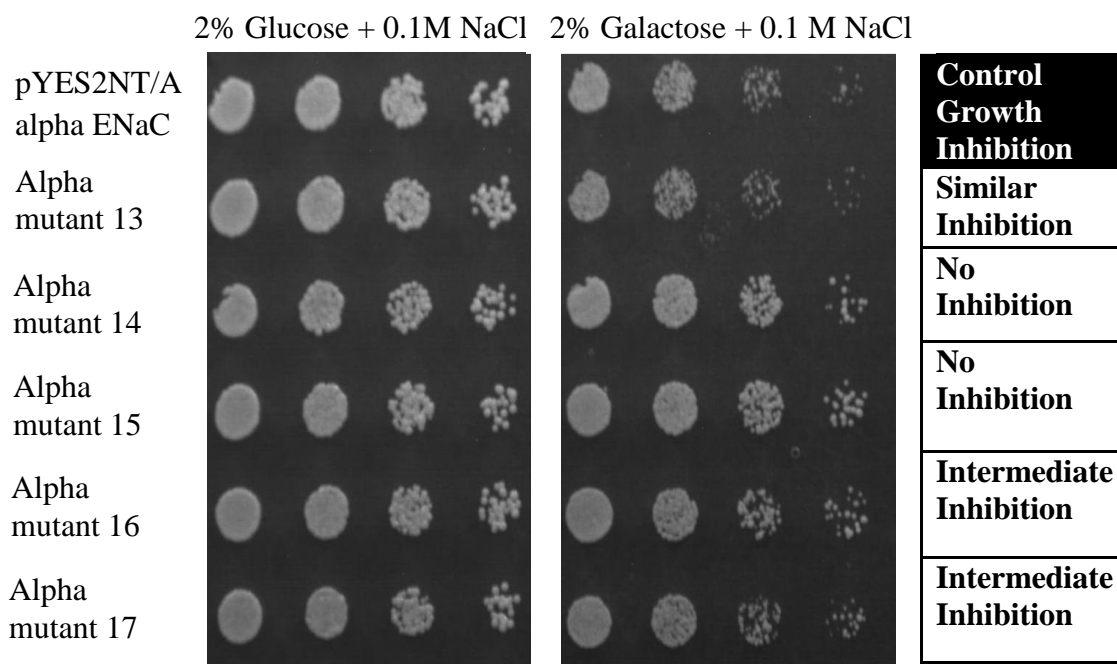


Figure 10: Dilution pronging assay of mutants and corresponding phenotype. S1InsE4A *S. cerevisiae* transformed with pYES2NT/A – alpha ENaC and EP-PCR mutants on synthetic media (2% w/v galactose + 0.1 M NaCl) showing growth inhibition. Samples of EP-PCR reactions 4, 5, and 6 correspond to alpha mutants 13-14, 15, and 16-17, respectively.

Table 4: Total phenotype observations for EP-PCR conditions

	Similar Growth Inhibition	Intermediate Growth Inhibition	No Growth Inhibition
Reaction #1	16	8	2
Reaction #2	2	1	0
Reaction #3	0	2	1
Reaction #4	2	0	1
Reaction #5	1	1	1
Reaction #6	1	1	1

Isolation of Mutant Plasmid from Yeast

Colonies of interest were inoculated into liquid 2% glucose minus Ura media and incubated at 30°C with shaking for 16 to 20 hours. Plasmid was isolated via the PrepEase

Yeast Plasmid Isolation kit. The resuspended plasmid then underwent gel electrophoresis for validation of isolation. Genomic and plasmid DNA are both present because they each precipitate ethanol during isolation (Figure 11). The plasmid is seen as a faint band at ~6 kb. Genomic DNA can be seen in the wells and degraded nucleic acid appears as the bright streaks throughout the gels. Even though not all of the plasmids are easily visualized within the lanes, they were nonetheless positively transformed in subsequent reactions. This has led us to believe that as long as there were plasmids present, being able to distinguish them on the gels are not necessarily required for identification of potential recombinant mutants.

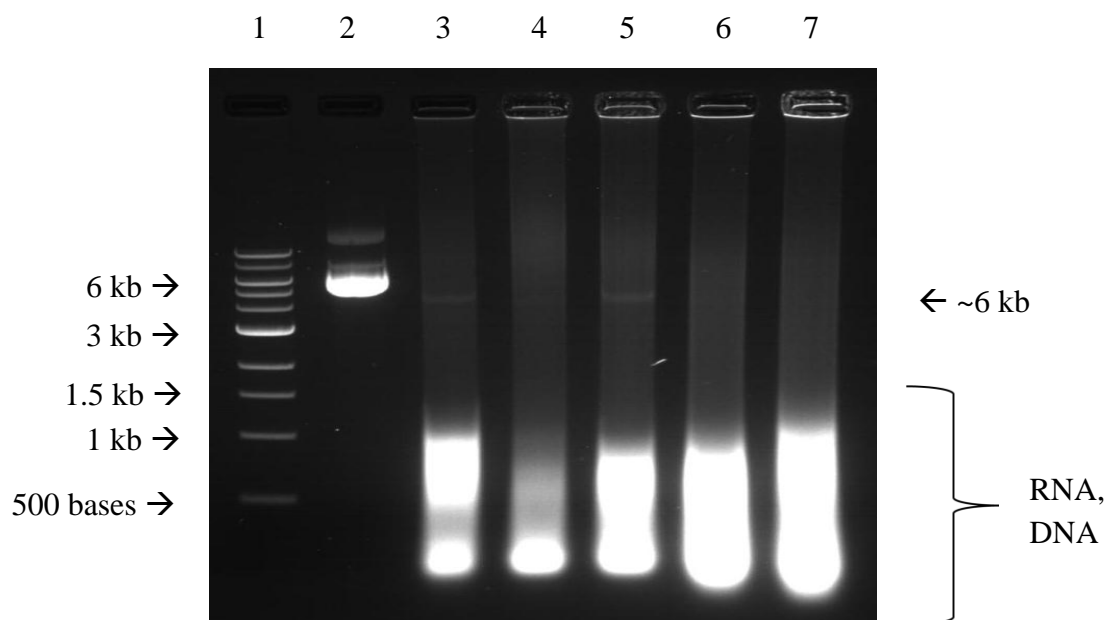


Figure 11: Gel electrophoresis of DNA isolated from *S. cerevisiae*. 1% Agarose gel in 1X TAE Buffer stained with Et Br. Lane 1- 1 kb DNA ladder, Lane 2- (control) pYES2NT/A – alpha ENaC, Lane 3- alpha mutant 4 (Reaction 1), Lane 4- alpha mutant 7 (Reaction 2), Lane 5- alpha mutant 10 (Reaction 3), Lane 6- alpha mutant 14 (Reaction 4), Lane 7- alpha mutant 15 (Reaction 5).

Mutant Plasmid Transformation into *E. coli*

Sequencing techniques required a 400 ng/ μ L to 500 ng/ μ L concentration of plasmids. Amplification of plasmids isolated from yeast was necessary to meet these requirements. The elution mixture from yeast contained plasmids, genomic DNA, and smaller nucleic acid sequences which gave a false high concentration reading from spectrophotometers. Adjustments to the heat shock transformation method were required since the concentration was unknown. Two microliters to 10 μ L of isolation mixture was added to competent Top 10 *E. coli* cells to empirically determine optimal transformation. Furthermore, 50 μ L to 500 μ L of transformation mixture was spread on LB agar plates with 100 μ g/ml ampicillin and incubated overnight at 37°C. Most positive results were from 5 μ L of DNA mixture and 200 μ L to 500 μ L spread aliquots, though they often consisted of very large colonies surrounded by satellites (Figure 12). Alpha mutant 10 (Figure 9 A) and alpha mutant 17 (Figure 9 B) were transformed with 5 μ L of yeast plasmid and each was grown from 500 μ L spreads onto the LB agar plates. Care was taken to avoid use of satellites and colonies that had grown together for downstream experiments.

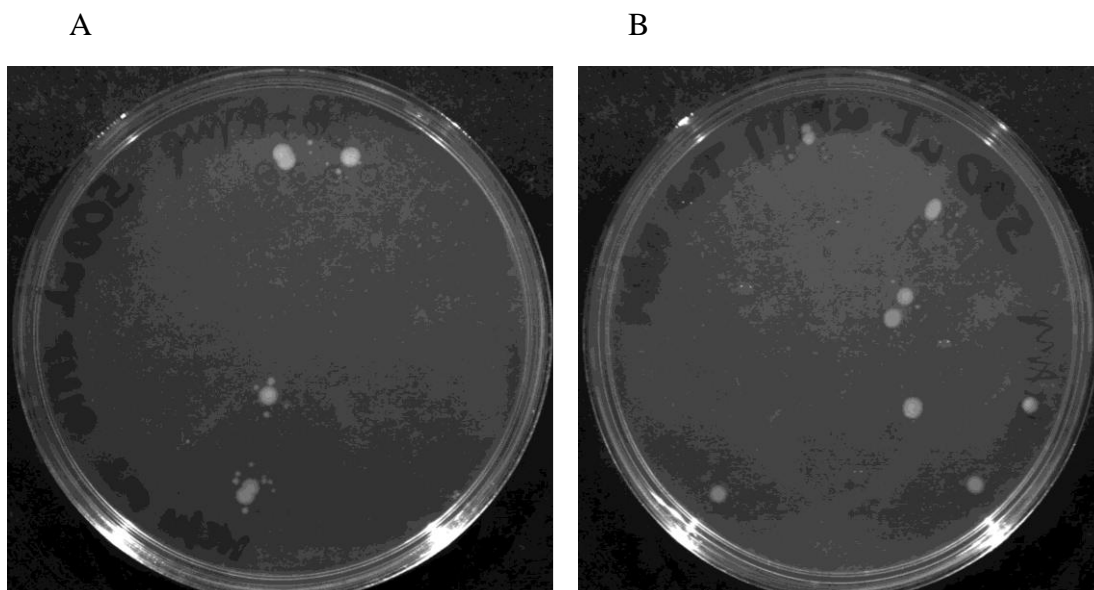


Figure 12: pYES2NT/A – alpha ENaC mutants transformed into *E. coli*. (A) Alpha mutant 10 containing two isolated colonies, two sets of overlapping colonies, and numerous satellite colonies. (B) Alpha mutant 17 containing six isolated colonies, two sets of overlapping colonies, and numerous satellites. Both plates are LB agar with 100 µg/mL ampicillin.

Mutant Plasmid Digestion

In order to validate EP-PCR insertion into pYES2NT/A – alpha ENaC the plasmids were isolated and digested with ClaI and AgeI. Three fragments were expected at 2079, 2737, and 3303 base pair. The digestion products were analyzed by horizontal gel electrophoresis. The fragments observed were ~2100, ~2700, and ~3300 base pair, thus, verifying that proper recombination occurred (Figure 13). Authentication was necessary because we observed instances of digested pYESNT/A – alpha ENaC that was ligated without EP-PCR product. The transformed yeast yielded a false positive because it was insusceptible to the selective media due to the fact that the improperly ligated

plasmid still conveyed resistance to minus Ura drop out media. Though, it did not express alpha ENaC.

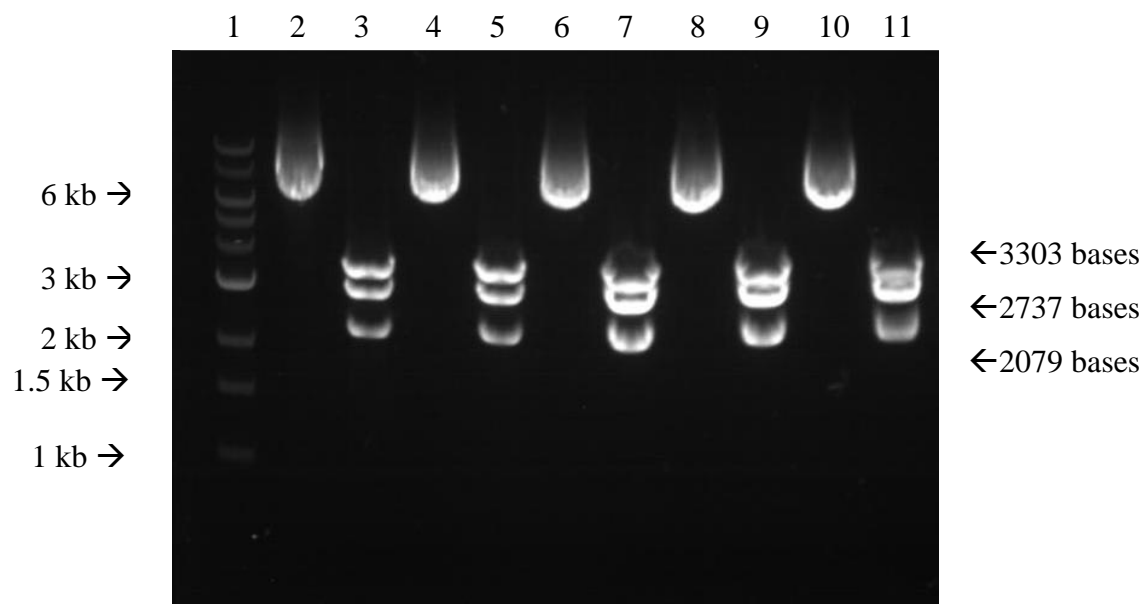


Figure 13: Digestion of mutant pYES2NT/A – alpha ENaC by *Cla*I and *Age*I. 1% Agarose gel in 1X TAE Buffer stained with Et Br. Lane 1- 1 kb ladder, Lane 2- uncut pYES2NT/A – alpha ENaC, Lane 3- digested pYES2NT/A – alpha ENaC, Lane 4- uncut alpha mutant 4, Lane 5- digested alpha mutant 4, Lane 6- uncut alpha mutant 7, Lane 7- digested alpha mutant 7, Lane 8- uncut alpha mutant 10, Lane 9- digested alpha mutant 10, Lane 10- uncut alpha mutant 14, Lane 11- digested alpha mutant 14.

Mutant Plasmid Sequencing

Mutants from pronging of each varied EP-PCR condition were selected to empirically discover the relative number of point mutations (Figure 14). Mutants that showed a lack of growth inhibition were selected, if present, for the initial sequencing reactions. Sequencing results were compared to wild-type *Mus musculus* SCNN1A

mRNA using Basic Local Alignment Search Tool (BLAST) bl2seq software (30), translated via the Swiss Institute of Bioinformatics tool (31), and compared to the wild-type *Mus musculus* SCNN1A amino acid sequence by BLAST (30). The optimal conditions were determined to be EP-PCR reactions 1 and 2, referring to alpha mutants 4 and 7, respectively. These reactions, which contained excessive magnesium ions only, displayed the fewest mutations as summarized by Table 3. Future pronging assays were centered on mutations created by reaction 1 in case the observed mutations due to reaction 2 were lower than normal based on the large deviation of mutations between reactions 2 and 3.

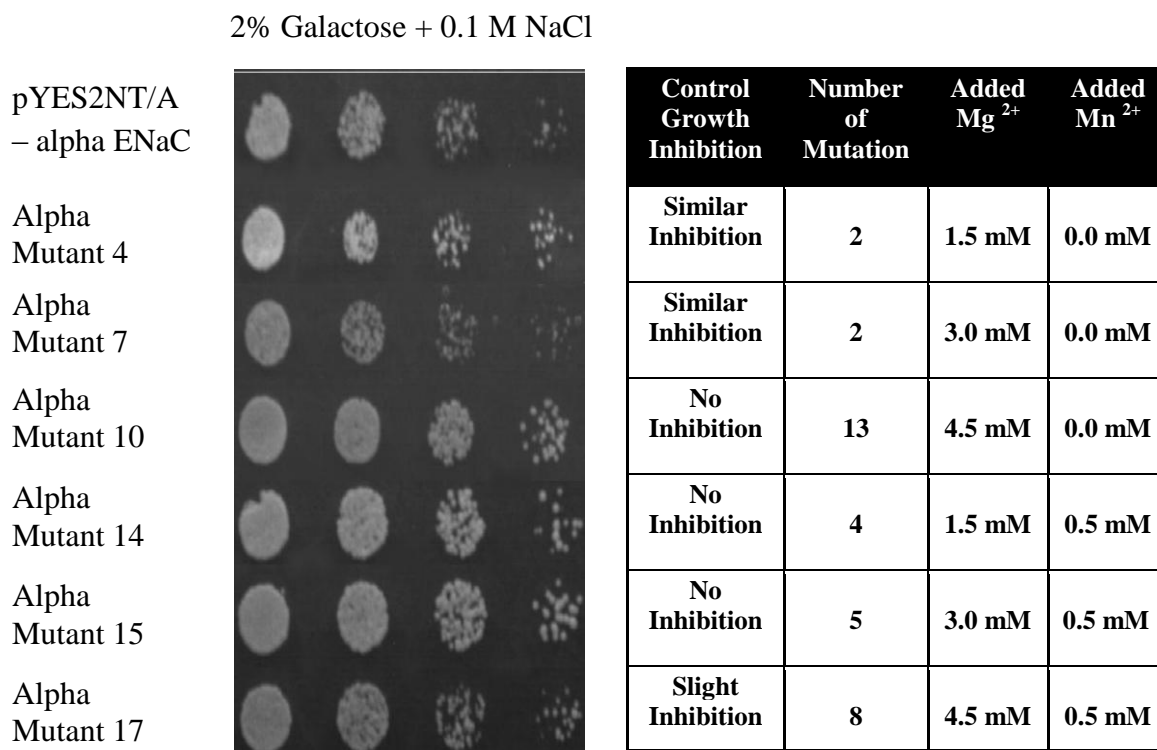


Figure 14: Pronging assay of each EP-PCR condition and point mutations.

Alignment of All Point Mutations

Eight mutated plasmids were sequenced. Common mutations found in the data were combined and compared to wild-type DNA to extrapolate the location of point mutations. The common mutations were superimposed to their corresponding loci and an alignment (Figure 15) was made using ClustalW software (32). It needs to be noted that the sequence for alpha ENaC is the sequence of the previously cloned vector which contained three point mutations that coded for silent mutations when translated: 1246 C→T, 1375 A→G, and 1822 T→C corresponding to S235S, E278E, and S427S, respectively.

```

alpha_ENaC      AAATACAACCTCTTCCTACACTCGCCAGGCTGGGGGCGCCGCCGCGCAGCACCCGCGACCTC
alphamutant15  AAATACAACCTCTTCCTACACTCGCCAGGCTGGGGGCGCCGCCGCGCAGCACCCGCGACCTC
alphamutant7    AAATACAACCTCTTCCTACACTCGCCAGGCTGGGGGCGCCGCCGCGCAGCACCCGCGACCTC
alphamutant53   AAATACAACCTCTTCCTACACTCGCCAGGCTGGGGGCGCCGCCGCGCAGCACCCGCGACCTC
alphamutant14   AAATACAACCTCTTCCTACACTCGCCAGGCTGGGGGCGCCGCCGCGCAGCACCCGCGACCTC
alphamutant4    AAATACAACCTCTTCCTACACTCGCCAGGCTGGGGGCGCCGCCGCGCAGCACCCGCGACCTC
alphamutant51   AAATACAACCTCTTCCTACACTCGCCAGGCTGGGGGCGCCGCCGCGCAGCACCCGCGACCTC
alphamutant17   AAATACAACCTCTTCCTACACTCGCCAGGCTGGGGGCGCCGCCGCGCAGCACCCGCGACCTC
alphamutant10   AAATACAACCTCTTCCTACACTCGCCAGGCTGGGGGCGCCGCCGCGCAGCACCCGCGACCTC
                *****

alpha_ENaC      CGGGGTGCTCTCCACACCCCCTGCAGCGCCTGCGCACACCACCTCCGCCAATCCCGCC
alphamutant15   CGGGGTGCTCTCCACACCCCCTGCAGCGCCTGCGCACACCACCTCCGCCAATCCCGCC
alphamutant7    CGGGGTGCTCTCCACACCCCCTGCAGCGCCTGCGCACACCACCTCCGCCAATCCCGCC
alphamutant53   CGGGGTGCTCTCCACACCCCCTGCAGCGCCTGCGCACACCACCTCCGCCAATCCCGCC
alphamutant14   CGGGGTGCTCTCCACACCCCCTGCAGCGCCTGCGCACACCACCTCCGCCAATCCCGCC
alphamutant4    CGGGGTGCTCTCCACACCCCCTGCAGCGCCTGCGCACACCACCTCCGCCAATCCCGCC
alphamutant51   CGGGGTGCTCTCCACACCCCCTGCAGCGCCTGCGCACACCACCTCCGCCAATCCCGCC
alphamutant17   CGGGGTGCTCTCCACACCCCCTGCAGCGCCTGCGCACACCACCTCCGCCAATCCCGCC
alphamutant10   CGGGGTGCTCTCCACACCCCCTGCAGCGCCTGCGCACACCACCTCCGCCAATCCCGCC
                *****

alpha_ENaC      CGCTCGGCGCGCAGCGCGTCTTCCAGTGTACGCGACAACAATCCCCAAGTGGACAGGAAG
alphamutant15   CGCTCGGCGCGCAGCGCGTCTTCCAGTGTACGCGACAACAATCCCCAAGTGGACAGGAAG
alphamutant7    CGCTCGGCGCGCAGCGCGTCTTCCAGTGTACGCGACAACAATCCCCAAGTGGACAGGAAG
alphamutant53   CGCTCGGCGCGCAGCGCGTCTTCCAGTGTACGCGACAACAATCCCCAAGTGGACAGGAAG
alphamutant14   CGCTCGGCGCGCAGCGCGTCTTCCAGTGTACGCGACAACAATCCCCAAGTGGACAGGAAG
alphamutant4    CGCTCGGCGCGCAGCGCGTCTTCCAGTGTACGCGACAACAATCCCCAAGTGGACAGGAAG
alphamutant51   CGCTCGGCGCGCAGCGCGTCTTCCAGTGTACGCGACAACAATCCCCAAGTGGACAGGAAG
alphamutant17   CGCTCGGCGCGCAGCGCGTCTTCCAGTGTACGCGACAACAATCCCCAAGTGGACAGGAAG
alphamutant10   CGCTCGGCGCGCAGCGCGTCTTCCAGTGTACGCGACAACAATCCCCAAGTGGACAGGAAG
                *****

```



```

alpha_ENaC      ATGCCTGGAGTCAACAATGGTTTGTCCCTGACACTGCGCACAGAGCAGAATGACTTCATC
alphamutant15  ATGCCTGGAGTCAACAATGGTTTGTCCCTGACACTGCGCACAGAGCAGAATGACTTCATC
alphamutant7    ATGCCTGGAGTCAACAATGGTTTGTCCCTGACACTGCGCACAGAGCAGAATGACTTCATC
alphamutant53  ATGCCTGGAGTCAACAATGGTTTGTCCCTGACACTGCGCACAGAGCAGAATGACTTCATC
alphamutant14  ATGCCTGGAGTCAACAATGGTTTGTCCCTGACACTGCGCACAGAGCAGAATGACTTCATC
alphamutant4    ATGCCTGGAGTCAACAATGGTTTGTCCCTGACACTGCGCACAGAGCAGAATGACTTCATC
alphamutant51  ATGCCTGGAGTCAACAATGGTTTGTCCCTGACACTGCGCACAGAGCAGAATGACTTCATC
alphamutant17  ACGCCTGGAGTCAACAATGGTTTGTCCCTGACACTGTGCACAGAGCAGAATGACTTCATC
alphamutant10  ATGCCTGGAGTCAACAATGGATTGTCCCTGACACTGCGCACAGAGCAGATTGACTTCATC
* ***** *

alpha_ENaC      CCCCTGCTGTCCACAGTGACGGGGGCCAGGGTGATGGTGCACGGTCAGGATGAGCCTGCT
alphamutant15  CCCCTGCTGTCCACAGTGACGGGGGCCAGGGTGATGGTGCACGGTCAGGATGAGCCTGCT
alphamutant7    CCCCTGCTGTCCACAGTGACGGGGGCCAGGGTGATGGTGCACGGTCAGGATGAGCCTGCT
alphamutant53  CCCCTGCTGTCCACAGTGACGGGGGCCAGGGTGATGGTGCACGGTCAGGATGAGCCTGCT
alphamutant14  CCCCTGCTGTCCACAGTGACGGGGGCCAGGGTGATGGTGCACGGTCAGGATGAGCCTGCT
alphamutant4    CCCCTGCTGTCCACAGTGACGGGGGCCAGGGTGATGGTGCACGGTCAGGATGAGCCTGCT
alphamutant51  CCCCTGCTGTCCACAGTGACGGGGGCCAGGGTGATGGTGCACGGTCAGGATGAGCCTGCT
alphamutant17  CCCCTGCTGTCCACAGTGACGGGGGCCAGGGTGATGGTGCACGGTCAGGATGAGCCTGCT
alphamutant10  CCCCTGCTGTCCACAGTGACGGGGGCCAGGGTGATGGTGCACGGTCAGGATGAGCCTGCT
* ***** *

alpha_ENaC      TTTATGGATGATGGTGGCTTCAACGTGAGGCCTGGTGTGGAGACCTCCATCAGTATGAGA
alphamutant15  TTTATGGATGATGGTGGCTTCAACGTGAGGCCTGGTGTGGAGACCTCCATCAGTATGAGA
alphamutant7    TTTATGGATGATGGTGGCTTCAACGTGAGGCCTGGTGTGGAGACCTCCATCAGTATGAGA
alphamutant53  TTTATGGATGATGGTGGCTTCAACGTGAGGCCTGGTGTGGAGACCTCCATCAGTATGAGA
alphamutant14  TTTATGGATGATGGTGGCTTCAACGTGAGGCCTGGTGTGGAGACCTCCATCAGTATGAGA
alphamutant4    TTTATGGATGATGGTGGCTTCAACGTGAGGCCTGGTGTGGAGACCTCCATCAGTATGAGA
alphamutant51  TTTATGGATGATGGTGGCTTCAACGTGAGGCCTGGTGTGGAGACCTCCATCAGTATGAGA
alphamutant17  TTTATGGATGATGGTGGCTTCAACGTGAGGCCTGGTGTGGAGACCTCCATCAGTATGAGA
alphamutant10  TTTATGGATGATGGTGGCTTCAACGTGAGGCCTGGTG--GAGACCTCCATCAGTATGAGA
* ***** *

alpha_ENaC      AAGGAAGCCCTGGACAGCCTCGGAGGCAACTACGGAGACTGCAC TGAGAATGGCAGCGAT
alphamutant15  AAGGAAGCCCTGGACAGCCTCGGAGGCAACTACGGAGACTGCAC TGAGAATGGCAGCGAT
alphamutant7    AAGGAAGCCCTGGACAGCCTCGGAGGCAACTACGGAGACTGCAC TGAGAATGGCAGCGAT
alphamutant53  AAGGAAGCCCTGGACAGCCTCGGAGGCAACTACGGAGACTGCAC TGAGAATGGCAGCGAT
alphamutant14  AAGGAAGCCCTGGACAGCCTCGGAGGCAACTACGGAGACTGCAC TGAGAATGGCAGCGAT
alphamutant4    AAGGAAGCCCTGGACAGCCTCGGAGGCAACTACGGAGACTGCAC TGAGAATGGCAGCGAT
alphamutant51  AAGGAAGCCCTGGACAGCCTCGGAGGCAACTACGGAGACTGCAC TGAGAATGGCAGCGAT
alphamutant17  AAGGAAGCCCTGGACAGCCTCGGAGGCAACTACGGAGTCTGCAC TGAGAATGGCAGCGAT
alphamutant10  GAGGAAGCCCTGGACAGCCTCGGAGGCAACTACGGAGGCTGCAC TGAGAATGGCAGCGAT
* ***** *

alpha_ENaC      GTCCCTGTCAAGAACCTTTACCCCTCCAAGTACACACAGCAGGTGTGCATTCACTCCTGC
alphamutant15  GTCCCTGTCAAGTACCTTTACCCCTCCAAGTACACACAGCAGGTGTGCATTCACTCCTGC
alphamutant7    GTCCCTGTCAAGAACCTTTACCCCTCCAAGTACACACAGCAGGTGTGCATTCACTCCTGC
alphamutant53  GTCCCTGTCAAGAACCTTTACCCCTCCAAGTACACACAGCAGGTGTGCATTCACTCCTGC
alphamutant14  GTCCCTGTCAAGAACCTTTACCCCTCCAAGTACACACAGCTGGTGTGCATTCACTCCTGC
alphamutant4    GTCCCTGTCAAGAACCTTTACCCCTCCAAGTACACACAGCAGGTGTGCATTCACTCCTGC
alphamutant51  GTCCCTGTCAAGAACCTTTACCCCTCCAAGTACACACAGCAGGTGTGCATTCACTCCTGC
alphamutant17  GTCCCTGTCAAGAACCTTTACCCCTCCAAGTACACACAGCAGGTGTGCATTCACTCCTGC
alphamutant10  GTCCCTGTCAAGAACCTTTACCCCTCCAAGTACACACAGCATGTGTGCATTCACTCCTGC
* ***** *

```

```

alpha_ENaC      TTCCAGGAGAACATGATCAAGAAGTGTGGCTGTGCCTACATCTTCTACCCTAAGCCCAAG
alphamutant15  TTCCAGGAGAACATGGTCAAGAAGTGTGGCTGTGCCTACATCTTCTACCCTAAGCCCAAG
alphamutant7    TTCCAGGAGAACATGATCAAGAAGTGTGGCTGTGCCTACATCTTCTACCCTAAGCCCAAG
alphamutant53  TTCCAGGAGAACATGATCAAGAAGTGTGGCTGTGCCTACATCTTCTACCCTAAGCCCAAG
alphamutant14  TTCCAGGAGAACATGATCAAGAAGTGTGGCTGTGCCTACATCTTCTACCCTAAGCCCAAG
alphamutant4    TTCCAGGAGAACATGATCAAGAAGTGTGGCTGTGCCTACATCTTCTACCCTAAGCCCAAG
alphamutant51  TTCCAGGAGAACATGATCAAGAAGTGTGGCTGTGCCTACATCTTCTACCCTAAGCCCAAG
alphamutant17  TTCCAGGAGAACATGATCAAGAAGTGTGGCTGTGCCTACATCTTCTACCCTAAGCCCAAG
alphamutant10  TTCCAGGAGAACATGATCAAGAAGTGTGGCTGTGCCTACATCTTCTACCCTAAGCCCAAG
*****

alpha_ENaC      GGTGTAGAGTTCTGTGACTACCTAAAGCAGAGCTCCTGGGGCTACTGCTACTATAAACTG
alphamutant15  GGTGTAGAGTTCTGTGACTACCTAAAGCAGAGCTCCTGGGGCTACTGCTACTATAAACTG
alphamutant7    GGTGTAGAGTTCTGTGACTACCTAAAGCAGAGCTCCTGGGGCTACTGCTACTATAAACTG
alphamutant53  GGTGTAGAGTTCTGTGACTACCTAAAGCAGAGCTCCTGGGGCTACTGCTACTATAAACTG
alphamutant14  GGTGTAGAGTTCTGTGACTACCTAAAGCAGAGCTCCTGGGGCTACTGCTACTATAAACTG
alphamutant4    GGTGTAGAGTTCTGTGACTACCTAAAGCAGAGCTCCTGGGGCTACTGCTACTATAAACTG
alphamutant51  GGTGTAGAGTTCTGTGACTACCTAAAGCAGAGCTCCTGGGGCTACTGCTACTATAAACTG
alphamutant17  GGTGTAGAGTTCTGTGACTACCTAAAGCAGAGCTCCTGGGGCTACTGCTACTATAAACTG
alphamutant10  GGTGTAGAGTTCTGTGACTACCTAAAGCAGAGCTCCTGGGGCTACTGCTACTATAAACTG
*****

alpha_ENaC      CAGGCTGCCT
alphamutant15  CAGGCTGCCT
alphamutant7    CAGGCTGCCT
alphamutant53  CAGGCTGCCT
alphamutant14  CAGGCTGCCT
alphamutant4    CAGGCTGCCT
alphamutant51  CAGGCTGCCT
alphamutant17  CAGGCTGCCT
alphamutant10  CAGGCTGCCT
*****

```

Figure 15: Alignment of sequenced mutant plasmids. The alignment displays a star beneath sites that exhibit homology between sequences.

The nucleotide sequences from each of the EP-PCR conditions were translated and summarized with their corresponding EP-PCR reaction, mutations, and growth pattern in yeast. Later experimentation involving the use of EP-PCR reaction 1 was also analyzed in a similar fashion and reported (Table 5).

Table 5: Summary of mutants, EP-PCR conditions, and amino acid transition

Alpha Mutant 4 (Reaction #1)	S233S and N353N	2 Silent Mutations	Similar Growth to Control
Alpha Mutant 7 (Reaction #2)	A231A and A234V	1 Silent 1 Non-Silent Mutations	Similar Growth to Control
Alpha Mutant 10 (Reaction #3)	L219R, S233S, R239R, R277(-), F312Y, N332Y, G355G, N365I, and *Deletion	Truncated Protein Frameshift and Nonsense Mutation	No Growth Inhibition
Alpha Mutant 14 (Reaction #4)	C310(-), P316P, Q442L, and G458C	Truncated Protein Nonsense Mutation	No Growth Inhibition
Alpha Mutant 15 (Reaction #5)	V273L and *Deletion	Truncated Protein Frameshift Mutation	No Growth Inhibition
Alpha Mutant 17 (Reaction #6)	H214R, N258S, F336S, M349T, R361C, P387P, G417S, and D421V	1 Silent 7 Non-Silent Mutations	Intermediate Growth Inhibition
Alpha Mutant 51 (Reaction #1)		0 Mutations	Similar Growth to Control
Alpha Mutant 53 (Reaction #1)		0 Mutations	Similar Growth to Control

Alpha mutant 4 possessed only silent mutations while alpha mutants 51 and 53 contained no mutations all of which correctly correspond to the yeast pronging assay phenotype of similar growth inhibition as the control. Alpha mutants 10, 14, and 15 each contained a nonsense mutation resulting in a premature stop codon and as a consequence the proteins were truncated. The truncated proteins would still be translated, but not

expressed on the cell surface due to a lack of C-terminal signaling sequences and rapid cytosolic degradation. This was consistent with the yeast screen as all three displayed no growth inhibition.

Alpha mutant 7 encoded one silent and one non-silent mutation. Alpha mutant 17 contained eight overall mutations with seven being non-silent. These two mutants were compared to the human alpha ENaC homology model and amino acid sequence alignment for identification of critical residues (Figure 16).

Because of the chemical similarities between alanine and valine A234V in alpha mutant 7 would not be likely to alter function to much extent. Also, a valine is conserved in human alpha ENaC at that position. These facts together with the observed growth inhibition similar to functional ENaC suggest A234V is not likely a critical mutation.

Alpha mutant 17 mutations H214R and N258S correspond to locations on the hyper-variable region (5). Because of the lack of conservation normally associated with this area, further testing will be required to determine the importance of these residues. Phenylalanine in F336S is highly conserved in all three human ENaC subunits and in

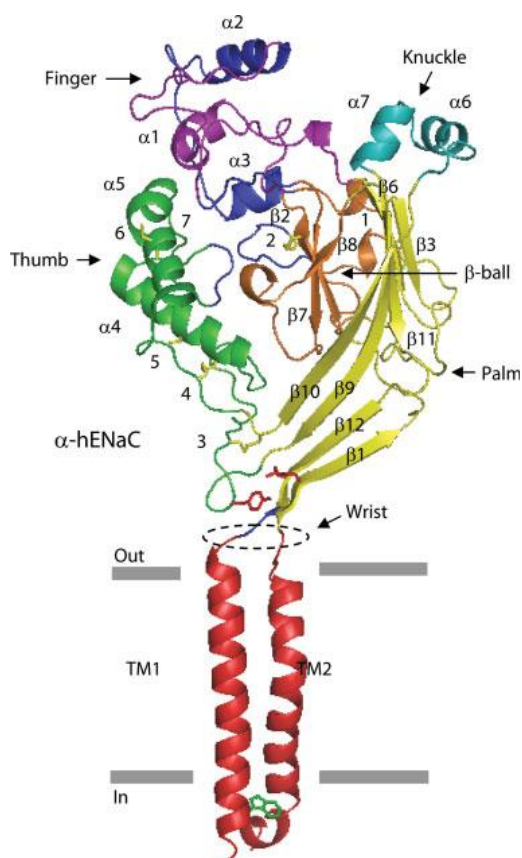


Figure 16: Model of human alpha ENaC based on the ASIC1 crystal structure. (5)

chicken ASIC1 it is located on the β 5 strand. However, human ENaC does not contain the β 5 strand thus jeopardizing the possible significance of this mutation. There is little conservation regarding M349T. The similarity in amino acid structure also may bring into question the importance of this mutation. R361C falls next to a highly conserved leucine residue on the B6 strand. The guanidinium group on the arginine side chain exhibits a positive charge in most biological environments and is capable of multiple hydrogen bonds which could play a role in inter- or intra-subunit assembly. G417S is proximal to a conserved tyrosine that is homologous to a tryptophan in ASIC1 known for being important to channel gating (33). Patch clamp studies regarding loss of function may be insightful for characterizing this mutation. D421V may be the most important mutation identified in alpha mutant 17 regarding subunit assembly. The mutation is juxtaposed to a conserved cysteine residue proposed to be responsible for integrity of subunit structure by intra-subunit bonding (5, 34).

Chapter IV

CONCLUSIONS

We hypothesized that a method could be developed to mutate specific regions of genes to analyze the importance of the corresponding amino acid residues to protein structure and function. The extracellular domain of alpha ENaC was the focus of the experiments presented in this study. Our method entails performing EP-PCR with primers that flank the protein region of interest. Subsequent genetic recombination of the mutations was achieved by the natural DNA repair mechanisms of *S. cerevisiae*. Yeast was also the model organism used to observe phenotypes corresponding to protein functionality. Mutated sequences were then analyzed to determine critical residue location.

By exploiting the absence of a 3' to 5' exonuclease proofreading mechanism in Taq polymerase and with addition of magnesium and manganese ions, known to increase error rate, we induced random mutations to the region of SCNN1A that codes for the extracellular loop of alpha ENaC. Incidents of mutation occurred much more frequently in the “combined” EP-PCR reactions. It determined that raising the magnesium concentration 1.5 mM or 3.0 mM in otherwise normal PCR conditions kept the number of mutations

to a minimum while simultaneously providing sufficient random mutagenesis for critical amino acid identification.

S. cerevisiae is a very effective model organism for characterizing mammalian proteins. Yeast cells, though sometimes able to tolerate significant amounts of salt, will experience cell growth inhibition when large quantities are absorbed (35). Based on this evidence a novel yeast screen was employed to describe phenotype alterations due to changes in ENaC structure and functionality from random mutagenesis.

Upon analysis of salt-sensitive phenotypes, mutated plasmids were sequenced and compared to the wild-type nucleotide sequence. We have identified a number of possibly critical mutations: R361C, G417S, and D421V. R361C possibly lost hydrogen bonding and/or ionic charge interactions between subunits by the guanidinium group on the arginine side chain because of replacement with the thiol group from cysteine. This may have conveyed a loss of function because of structural instability. The glycine on position 417 and others surrounding the conserved tyrosine allow for flexibility within the “wrist” of ENaC and when altered to serine may have impeded on the functionality of the channel. Recent studies corroborate this by mutations to the other proximal glycines (36). D421V is juxtaposed to a conserved cysteine that forms a disulphide bridge within the subunit. The aspartate may be involved with intrasubunit interactions based on known intrasubunit bonding employed by the cysteine. The alteration of the charged aspartate group to a nonpolar valine may have caused a loss of function due to structural changes or weakened stability of the subunit.

The number and type of mutations occurred during translation of alpha ENaC correctly corresponded to the phenotypes observed in the yeast dilution pronging assay. This confirmation supports the future use of our method for inducing mutations and describing the conveyed phenotypes for prediction of genes that may contain critical mutations.

REFERENCES

1. Post R., Sen A., and Rosenthal A. *J Biol Chem* **1965**, 240, 1437-45.
2. Canessa C. M., Schild L., Buell G., Thorens B., Gautschi I., Horisberger J. D., and Rossier B. C. *Nature* **1994**, 367, 463-67.
3. Kellenberger S. and Schild L. *Physiol Rev* **2002**, 82, 735–67.
4. Staruschenko A., Adams E., Booth R. E., and Stockand J. D. *Biophys. J.* **2005**, 88, 3966–75.
5. Stockand J. D., Staruschenko A., Pochynyuk O., Booth R. E., and Silverthorn D. U. *IUBMB Life* **2008**, 60, 620-8.
6. Harris M., *et al.* *J. Biol. Chem.*, **2008**, 283, 7455-63.
7. Canessa C. M., Horisberger J. D., and Rossier B. C. *Nature* **1993**, 361, 467–70.
8. Firsov D., Gautschi I., Merillat A. M., Rossier B. C., and Schild L. *EMBO J* **1998**, 17, 344-52.
9. McNicholas C. and Canessa C. *J Gen Physiol* **1997**, 109, 681-92.
10. Snyder P. M. *Endocrine Reviews* **2002**, 23, 258-275.
11. Wilson Y., Nag N., Davern P., Oldfield B. J., McKinley M. J., Greferath U., and Murphy M. *Proc Natl Acad Sci U S A* **2002**, 99, 3252 –57.
12. Sofroniew M. V. in *Handbook of Chemical Neuroanatomy*, eds Björklund A. and Hökfelt T. (Elsevier, Amsterdam) **1985**, 4, pp 93–165.
13. Knepper M. A., Nielsen S., Chou C. L., and DiGiovanni S. R. *Semin. Nephrol* **1994**, 14, 302–21.
14. Butterworth M. B., Frizzell R. A., Johnson J. P., Peters K. W., and Edinger R. S. *Am J Physiol Renal Physiol* **2005**, 289, 969–77.

15. Li C., Wang W., Rivard C. J., Lanaspá M. A., Summer S., and Schrier R. W. *Am J Physiol Renal Physiol* **2011**, 300, 1255-61.
16. Masilamani S., Kim G. H., Mitchell C., Wade J. B., and Knepper M. A. *J Clin Invest* **1999**, 104, R19-R23.
17. May A., Puoti A., Gaeggeler H. P., Horisberger J. D., and Rossier B. C. *J Am Soc Nephrol* **1997**, 8, 1813-22.
18. Debonneville C., Flores S. Y., Kamynina E., Plant P. J., Tauxe C., Thomas M. A., Munster C., Chraïbi A., Pratt J. H., Horisberger J. D., Pearce D., Loffing J., and Staub O. *EMBO J* **2001**, 20, 7052-59.
19. Snyder P. M., Olson D. R., and Thomas B. C. *J Biol Chem* **2002**, 277, 5-8.
20. Liang X., Peters K., Butterworth M., and Frizzel R. *J Biol Chem* **2006**, 281, 16323-32.
21. Yanase M. and Handler J. *Am J Physiol Cell Physiol* **1986**, 250, 517-22.
22. Booth R. and Stockand J. *Am J Physiol Renal Physiol* **2003**, 284, 938-47.
23. Staub O. *EMBO J* **1997**, 16, 6325-36.
24. Glickman M. and Ciechanover A. *Physiol Rev* **2002**, 82, 373-428.
25. Niemeyer B. A., *et al.* *EMBO Reports* **2001**, 2, 568-73.
26. Boucher R. C., Stutts M. J., Knowles M. R., Cantley L., and Gatzky J. T. *J. Clin. Invest.* **1986**, 78, 1245-52.
27. Hanukoglu A. *J Clin Endocrinol Metab* **1991**, 73, 936-44.
28. Ma H., Kunes S., Schatz P.J., and Botstein D. *Gene* **1987**, 55, 201-16.
29. Oldenburg K. R., Vo K. T., Michaelis S., and Paddon C. *Nucleic Acids Res* **1997**, 25, 451-52.
30. Altschul S. F., Gish W., Miller W., Myers E. W., and Lipman D. J. *J. Mol. Biol.* **1990**, 215, 403-10.
31. Gasteiger E., Gattiker A., Hoogland C., Ivanyi I., Appel R. D., and Bairoch A. *Nucleic Acids Res* **2003**, 31, 3784-88.
32. Larkin M. A., Blackshields G., Brown N. P., Chenna R., McGettigan P. A., McWilliam H., Valentin F., Wallace I. M., Wilm A., Lopez R., Thompson J. D., Gibson T. J. and Higgins D. G. *Bioinformatics* **2007**, 23(21), 2947-48.

33. Li T., Yang Y., Canessa C. M. *J Biol Chem* **2009**, 284, 4689–94.
34. Jasti J., Furukawa H., Gonzales E., and Gouaux E. *Nature* **2007**, 449, 316-23.
35. Haass F. A., Jan L. Y., and Shulder M. *PNAS* **2007**, 104, 18079-84.
36. Shi S., Ghosh D. D., Okumura S., Carattino M. D., Kashlan O. B., Sheng S., and Kleyman T. R. *J Biol Chem* **2011**, 286, 14753-61.

VITA

Ty Whisenant was born in Canyon, TX, on March 10, 1983 to Lyndon and Tana Whisenant. He grew up in Canyon and successfully graduated from Canyon High School in 2001. Ty initially attended West Texas A&M University and completed his undergraduate degree at Texas Tech University. He graduated with a Bachelor of Arts in Biological Chemistry in May of 2006. Following graduation Ty was employed as a Quality Control Chemist at Texas Industries for two years in Midlothian, TX. He was subsequently employed as contractor for military and healthcare operations in the Austin, TX area. In the Fall semester of 2009 Ty entered the Biochemistry Graduate Program at Texas State University San Marcos under the direction of Dr. Rachell E. Booth.

Permanent Email Address: ty.whisenant@hotmail.com

This thesis was typed by Ty E. Whisenant.